Class-C transistor power amplifier," Ph.D. dissertation, Carleton Univ., Ottawa, Canada, 1976.
[8] S. R. Mazumder and P. D. van der Puije, "Characterization of non-linear 2-ports for the design of Class-C amplifiers," *IEE J. Microwaves Optics Acoust.*, vol. 1 no. 4, pp. 138–142, July 1977.
[9] —, "An experimental method of characterizing non-linear 2-ports and its application to microwave Class-C transistor power amplifier design," *IEEE J. Solid-State Circuits*, vol. SC-12, pp. 576–580, Oct. 1977.
[10] R. Saal and E. Ulbrich, "On the design of filters by synthesis," *IRE Trans. Circuit Theory*, pp. 284–327, Dec. 1958.
[11] Y. Takayama, "A new load-pull characterization method for microwave power transistors," in *Digest Tech. Papers, 1976 IEEE MTT-S Int. Microwave Symp.*, pp. 218–220.

Cavity Stabilization and Electronic Tuning of a Millimeter-Wave IMPATT Diode Oscillator by Parametric Interaction

HIROSHI OKAMOTO, MEMBER, IEEE, AND MUTSUO IKEDA

***Abstract*—A new technique is proposed by which both noise reduction and electronic tuning of a millimeter-wave solid-state oscillator can be realized by injecting an arbitrary low-frequency (several hundred megahertz or beyond) signal to the oscillator element which is provided with an additional high-Q cavity.**

This method has much wider tuning bandwidth than that of the conventional subharmonic injection locking technique.

Presented are both experimental results and some theoretical interpretations by using an IMPATT diode oscillator.

I. Introduction

INJECTION LOCKING is a conventional circuit technology to reduce sideband noise and to give electronic tunability to solid-state oscillators. Three types of injection locking methods have been developed by now. They are as follows.

1) Fundamental-wave injection locking [1]—Here, the frequency of the injection signal f_{inj} is nearly equal to the free-running oscillation frequency f_O to be locked.

2) Subharmonic injection locking [2]—Here, f_{inj} is nearly equal to $(1/n)\cdot f_O$, where n is an integer larger than unity.

3) Sideband-wave injection locking [3]—Here, two injection signals are used, one of which is a low-frequency signal $f_{inj,\,1}$, and the other a signal with frequency $f_{inj,\,2} \doteqdot f_O \pm f_{inj,\,1}$.

The first and the third techniques have wider locking bandwidth (i.e., tuning bandwidth) than the second, when compared for a particular gain. With increasing frequency, however, it becomes more difficult to realize a low-noise injection signal source with frequency nearly equal to that of the oscillator to be stabilized.

The advantage of the second technique is that a low-frequency signal can be used for injection. But unfortunately, the tuning bandwidth becomes narrower when the order of multiplication n is increased. In one example of the subharmonic injection locking of an 8.5-GHz IMPATT diode oscillator, it was reported [2] that the available tuning bandwidth is 1 MHz or less when n is equal to 9 and the locking gain is 0 dB.

In order to overcome these difficulties, a new technique is proposed here, which is an extended version of the injection locking technique to a parametrically interacting system. This method has the following two advantages.

1) The frequency of the injection signal can be selected somewhat arbitrarily (at several hundred megahertz or beyond). We can, therefore, use an injection signal whose frequency is much lower than that of the solid-state oscillator to be stabilized. This makes it rather easy to realize the injection signal source.

2) The tuning bandwidth is much wider than that provided by subharmonic injection locking. The bandwidth is comparable to that obtainable with fundamental-wave and sideband-wave injection locking methods.

Experimental results on a millimeter-wave IMPATT diode oscillator are presented in this paper, along with some analytical discussions.

II. Mechanism

The frequency planes shown in Fig. 1 illustrate the mechanism of the new technique discussed here.

Assume an IMPATT diode oscillator is oscillating freely at f_O. This is shown in Fig. 1(a). The frequency f_O is

Manuscript received August 22, 1977; revised December 20, 1977.

The authors are with the Musashino Electrical Communication Laboratory, Nippon Telegraph and Telephone Public Corporation, Musashino-shi, Tokyo 180, Japan.

0018-9480/78/0600-0420$00.75

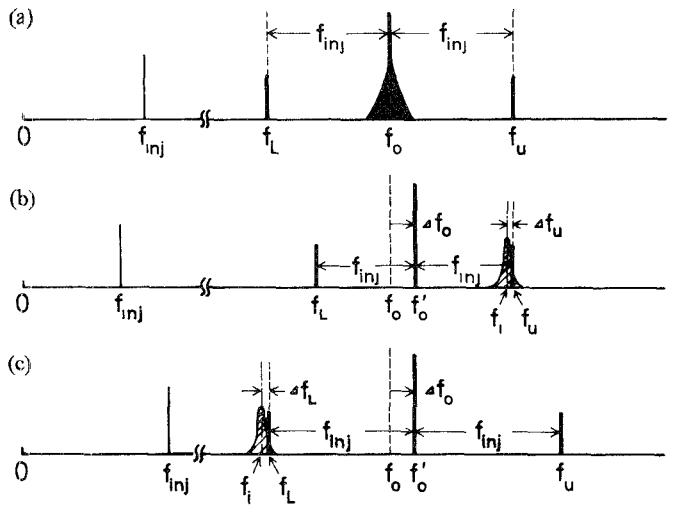

Fig. 1. Spectral representation of the stabilization and tuning method presented here. (a) A free-running state with low-frequency signal f_{inj} injected. No idler cavity is provided. (b) The upper sideband trapping. The idler cavity f_i captures the upper sideband frequency f_u. (c) The lower sideband trapping. The idler cavity f_i traps the lower sideband frequency f_L.

determined by the main resonator such as a cap-type resonator. Coupled to the main resonator is another high-Q cavity resonator which is called an idler resonator, and its resonant frequency is f_i. f_i is a few gigahertz away from f_O. When injecting a signal whose frequency is nearly equal to the difference frequency between f_O and f_i, many sideband components are produced, whose frequencies are $f_u = f_O + f_{inj}$ (upper sideband), $f_L = f_O - f_{inj}$ (lower sideband), etc. Due to the presence of the high-Q idler cavity, one of these frequencies f_u or f_L, whichever is nearer to the resonant frequency f_i, is trapped by that cavity and is held constant, although the injection signal frequency f_{inj} may be varied. As a consequence, the oscillation frequency begins to change directly in relationship to the change in f_{inj}. The difference between the new oscillation frequency f_O' and the trapped-sideband frequency is always equal to f_{inj}. Due to the large Q of the idler cavity, the sideband noise of f_O' is drastically reduced, compared to that in the free-running state.

Fig. 1(a) shows the free-running state with an injected low-frequency signal. An idler cavity is not provided here, so that the noise is not reduced and the oscillation frequency is not dependent upon f_{inj}. Figs. 1(b) and (c) show the locked states realized by the present method. A locked state refers here to a state where the aforementioned mechanism is operating. The idler cavity is shown by a Q curve centered at f_i. In the case of (b), the idler cavity captures the upper sideband frequency f_u. This case is called upper sideband trapping. In the case of (c), the cavity traps the lower sideband frequency f_L. This case is called lower sideband trapping.

As shown in this figure, shifts in frequencies of the oscillation, the upper sideband, and the lower sideband signals are defined, respectively, by

$$\Delta f_O = f_O' - f_O$$
$$\Delta f_u = f_u - f_i$$
$$\Delta f_l = f_l - f_i.$$

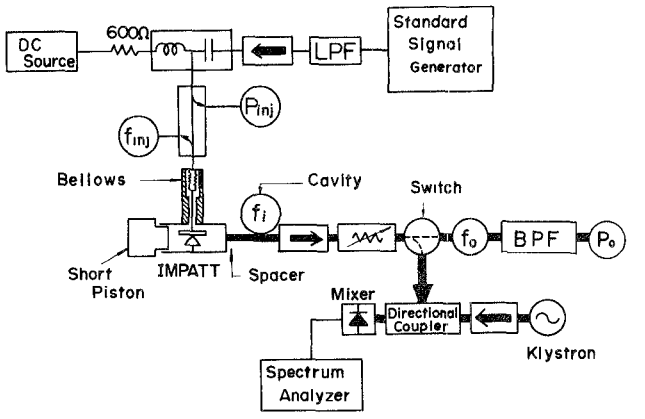

Fig. 2. Experimental circuit.

III. Experiment

Fig. 2 is the experimental circuit used to demonstrate the method presented here.

A GaAs Schottky-barrier IMPATT diode is used as an oscillating element. Its free-running frequency f_O is 36.7 GHz and its output power P_O is 19.2 dBm. A conventional cap-type resonator is used as the main cavity, whose external Q is 50–100.

An idler cavity resonator is located at nearly 4 λ_g away from the diode. The resonant mode is a cylindrical TE_{011}, and its Q is 1500–2000. A low-frequency signal is injected through the bias circuit of the IMPATT oscillator. Its power P_{inj} and frequency f_{inj} are monitored at a point close to the diode mount.

The output power P_O of the oscillation is measured through a bandpass filter to reject the power of the sideband components.

A spectrum analyzer is used to measure the spectral power distribution, and it was found out that the power of any of the sideband components is at least 10 dB below the oscillation output power P_O.

In order to accurately measure the frequency shifts Δf_O, Δf_u, and/or Δf_L, the relevant frequencies are down converted and measured with the spectrum analyzer or a frequency counter.

Fig. 3 shows an example of the tuning characteristics in the case of the upper sideband trapping. The resonant frequency of the idler cavity f_i is selected at 1400 MHz above f_O. Here the injection signal frequency f_{inj} is varied while keeping its power P_{inj} constant at 5 dBm.

If f_{inj} is decreased from 1400 MHz, Δf_O increases with a constant slope of -1, while Δf_u approaches asymptotically to a constant value. The asymptotic value could not be determined accurately, due to the limited accuracy of our measuring setup.

When f_{inj} increases beyond 1400 MHz, Δf_O remains at or nearly equal to zero and no locked state exists, although not shown in this figure. It is noticeable that the oscillation frequency in the locked state is always higher than that in the free-running state; i.e., $\Delta f_O > 0$. The output power P_O at the oscillation frequency decreases by less than 1 dB over the tuning bandwidth of 180 MHz in this example. In addition, power gain P_O/P_{inj} of 13 dB is available.

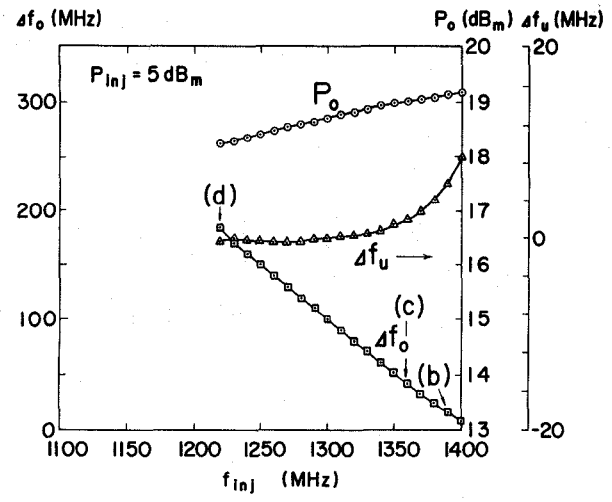

Fig. 3. An example of tuning properties for the upper sideband trapping. $f_i = f_O + 1400$ MHz. Arrows (b), (c), and (d) correspond to photographs (b), (c), and (d) shown in Fig. 4, respectively.

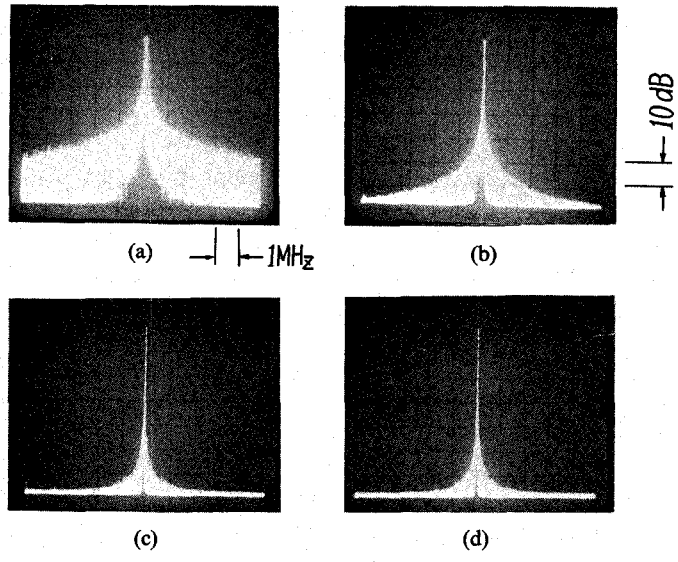

Fig. 4. Spectra of the oscillation signal. Horizontal—1 MHz/div. Vertical—10 dB/div. (a) A free-running state. (b), (c), and (d) The locked states which are represented by arrows (b), (c), and (d), respectively, shown in Fig. 3.

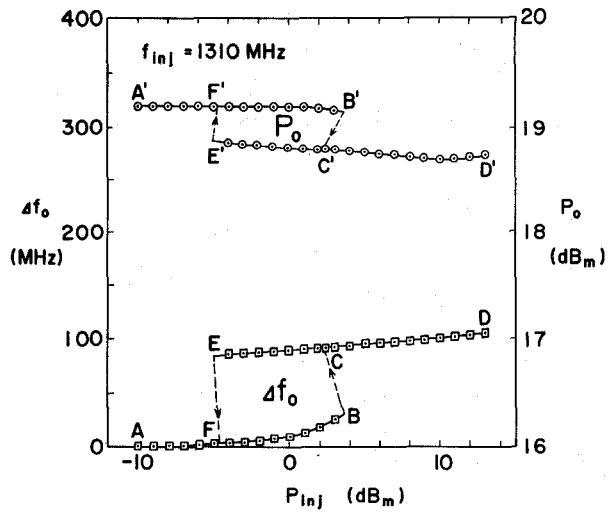

Fig. 5. Frequency shift Δf_O and output power P_O as a function of injection signal power P_{inj} in the upper sideband trapping. $f_i = f_O + 1400$ MHz. $A(A')-F(F')-B(B')$—unlocked state. $E(E')-C(C')-D(D')$—locked state.

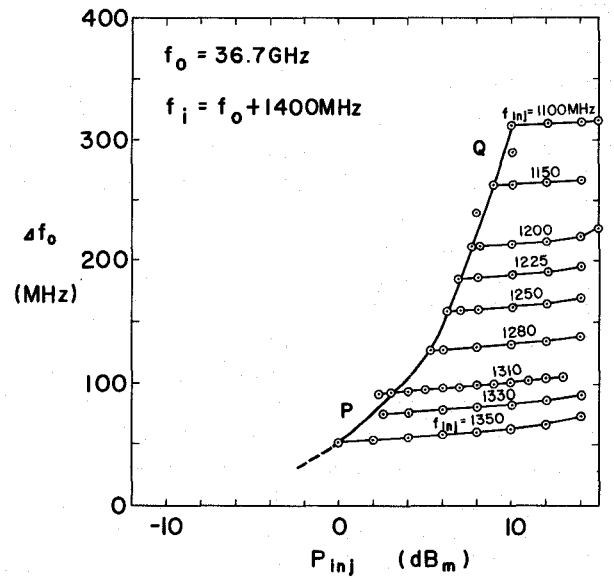

Fig. 6. Locked states and tuning critical curve for the upper sideband trapping. $f_i = f_O + 1400$ MHz.

Spectra of the oscillation signal are shown in Fig. 4.(a) is the spectrum in the free-running state. Figs. 4(b), (c), and (d) are those in the locked states at the points (b), (c), and (d), respectively, shown in Fig. 3. In all of the spectra in Fig. 4, the horizontal scale is 1 MHz/div and the vertical scale is 10 dB/div. The bandwidth of the spectrum analyzer is 10 kHz. By comparing the noise level at, for example, 1-MHz off carrier between the spectra (a) and (c) or (d), it is clear that the sideband noise in the locked state is lower than that in the free-running state by more than 25 dB. The low noise state is maintained between the points (c) and (d).

In Fig. 5, the frequency shift Δf_O and the output power P_O are plotted as a function of the injection signal power P_{inj}. The injection signal frequency f_{inj} is kept constant at 1310 MHz. When increasing P_{inj}, the characteristics follow the locus $A(A')-B(B')-C(C')-D(D')$. The locked state starts at the point $C(C')$ and continues to $D(D')$. When decreasing P_{inj}, the locked state is maintained until the point $E(E')$ is reached; here a jump occurs to the point $F(F')$, whereupon the oscillator returns to the unlocked state. Hysteresis is always observed in the transition region between the locked state and the unlocked one.

The portion $C(C')-D(D')$ in Fig. 5 represents locked states which are not influenced by the hysteresis. Δf_O versus P_{inj} curves in these locked states, one of which is shown by the curve C–D in Fig. 5, are depicted in Fig. 6 for various values of f_{inj} as a parameter. The curve P–Q, which is a trajectory of the point C in Fig. 5, shows that the tuning bandwidth increases nearly in proportion to the injection signal power P_{inj}. The maximum tuning bandwidth obtained here is 320 MHz. This is much larger than that obtained by the subharmonic injection locking [2],

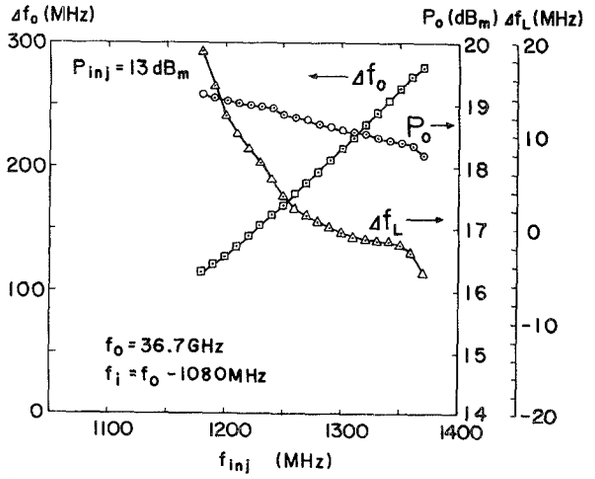

Fig. 7. An example of tuning properties for the lower sideband trapping. $f_i = f_O - 1080$ MHz.

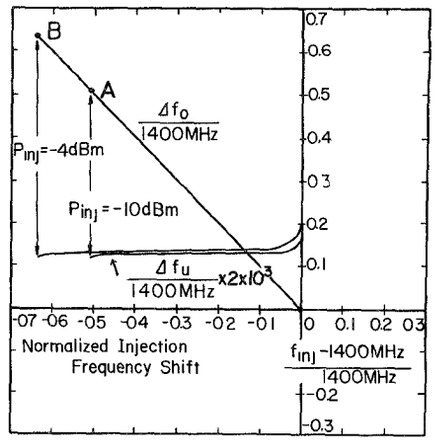

Fig. 8. Computed results of tuning properties for the upper sideband trapping.

and is comparable to those of the fundamental-wave [1] and the sideband-wave injection locking circuits [3], although direct comparison must be made under the same value of Q.

An example of the experimental results on the lower sideband trapping is shown in Fig. 7, where the frequency of the idler cavity is set at 1080-MHz below f_O. The injection power P_{inj} is kept constant at 13 dBm. The tuning properties are similar to those for the previous case except on the following two points.

1) When increasing f_{inj}, Δf_O increases with a constant slope of $+1$, instead of -1, and P_O decreases little by little.

2) The asymptotical behavior of Δf_L is not as pronounced as that of Δf_u in the previous case.

The tuning bandwidth in this example is 170 MHz, and its maximum of 250 MHz is obtained with P_{inj} equal to $\sim$15 dBm.

It is noted that $\Delta f_O > 0$, or the oscillation frequency in the locked state is again higher than that in the free-running state. This means that the tuning range of the present technique is asymmetric, since it lies only on the higher frequency side of the free-running frequency f_O in both upper and lower sideband trapping cases. Here, we recall that with the fundamental-wave and the subharmonic injection locking circuits, the tuning (locking) ranges occur essentially symmetrically with respect to the free-running frequency f_O.

IV. Theoretical Approach

In order to treat the present technique from the circuit theoretical point of view, a three-frequency parametric interaction model is adopted here. We restrict ourselves only to the upper sideband trapping case. Theoretical procedures taken are as follows.

1) The first step is to describe analytically the three-frequency system: the oscillation frequency f_O', the injection frequency f_{inj}, and the upper sideband (idler) frequency f_u. These three signals interact mutually through the nonlinear avalanche inductance of the IMPATT diode. For each of the three frequencies, equivalent circuits are obtained from the general representation given by Gupta [4] for the Read model of an IMPATT diode.

2) In the next step, the basic principle on the theory of the fundamental-wave injection locking developed by Kurokawa [1] is extended to this three-frequency system. From this, we can derive expressions for the tuning properties, the stability criterion, and the noise reduction factor.

3) Finally, a computation is performed by applying the theory to the experiment just described. The detail of these procedures requires rather lengthy description, which will be published elsewhere [5], so that only the essential part of the analysis is given below.

Fig. 8 shows the tuning properties that are computed for the case of $f_i = f_O + 1400$ MHz. The normalized oscillation frequency shift $\Delta f_O/1400$ MHz and the normalized upper sideband (idler) wave frequency shift $\Delta f_u/1400$ MHz are shown as a function of the normalized injection frequency shift $(f_{inj} - 1400\ \text{MHz})/1400$ MHz. The injection power level P_{inj} is a parameter.

When P_{inj} is equal to -10 dBm, for example, Δf_O changes almost linearly with a slope of -1 from the origin to the point A when decreasing f_{inj}, while Δf_u is kept almost constant. There are no stable locked states outside the range $-0.51 \leqslant (f_{inj} - 1400\ \text{MHz})/1400\ \text{MHz} \leqslant 0$, which is, therefore, the tuning range expressed in terms of the injection frequency.

Although not shown in this figure, the output power at the oscillation frequency f_O' in the locked state is computed to be lower by only a small amount (0.02 dB or below) than that in the free-running state. For the case of $P_{inj} = -4$ dBm, the locked states are represented by the line from the origin to the point B. The tuning range in this case is $-0.64 \leqslant (f_{inj} - 1400\ \text{MHz})/1400\ \text{MHz} \leqslant 0$.

As can be seen, all of the qualitative features observed in the experiment:

1) the tuning range is asymmetrical with respect to f_O, or $\Delta f_O > 0$,

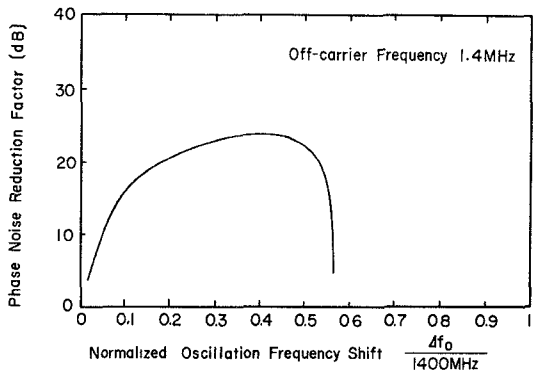

Fig. 9. Phase noise reduction factor versus normalized frequency shift of the oscillation signal. (Computed result.)

2) Δf_O is linearly dependent on the change of f_{inj}, or $\partial \Delta f_O / \partial f_{inj} \fallingdotseq -1$,
3) Δf_u is nearly insensitive to the change of f_{inj},
4) the tuning range is an increasing function of P_{inj},
5) the output power at f_O' in the locked state is lower than that in the free-running state,

are well explained by the theory.

The phase noise reduction factor is defined here as a ratio of the phase noise of the oscillation signal in the free-running state to that in the locked state. This factor calculated at the off-carrier frequency of 1.4 MHz is shown in Fig. 9 as a function of the normalized oscillation frequency shift $\Delta f_O/1400$ MHz for the case of $P_{inj} = -7$ dBm. As can be seen, this reduction factor increases with increasing Δf_O, reaches a maximum of 23 dB and then decreases at the end of the tuning range. This property is also in good agreement with the experimental result shown in Fig. 4.

V. Application

The following are three applications of this stabilization and tuning method, which are considered to be important.

1) Low-noise oscillator with electronic tunability—This can be easily realized if an electronically tunable injection signal source is used.

2) Low-noise oscillator with high stability—This can be realized by picking up a part of the oscillation signal and supplying it to a frequency discriminator. The output of the discriminator is proportional to a drift $\delta f_O'$ in the oscillation frequency, and it is fed back to the injection signal source in such a way that f_{inj} is changed so as to cancel the drift $\delta f_O'$ [6].

3) Up-converter with power gain of an FM-modulated intermediate frequency signal—This application is based on the linear relationship between the injection (input) signal frequency f_{inj} and the oscillation (output) signal frequency f_O' shown in Figs. 3 and 7.

VI. Conclusion

A new method is proposed for noise reduction and electronic tuning of a millimeter-wave solid-state oscillator. This method utilizes the parametric interaction which is caused by providing a high-Q idler cavity in the vicinity of an oscillating element and by injecting a signal whose frequency is much lower than the oscillation frequency. An experimental demonstration using a GaAs IMPATT diode oscillating at 37 GHz shows that the tuning range of more than 300 MHz can be obtained, which is much wider than that obtained by using the subharmonic injection locking method. Theoretical analysis is also presented, which qualitatively explains the experimental results. Some applications are also proposed.

Acknowledgment

The authors wish to thank Dr. M. Fujimoto, Dr. Y. Sato, and Dr. M. Watanabe for their continuous encouragement. They are also indebted to Prof. J. Hamasaki of the University of Tokyo, for many suggestions and discussions throughout this study.

References

[1] K. Kurokawa, "Injection locking of microwave solid-state oscillators," *Proc. IEEE*, vol. 64, pp. 1386–1410, Oct. 1973.
[2] C. H. Chien and G. C. Dalman, "Subharmonically injection phase-locked IMPATT oscillator experiments," *Electron. Lett.*, vol. 6, pp. 240–241, Apr. 1970.
[3] Y. Fukatsu and H. Kato, "Frequency conversion with gain through sideband locking of an IMPATT diode oscillator," *Proc. IEEE*, vol. 57, pp. 342–343, Mar. 1969.
[4] M. S. Gupta, "A nonlinear equivalent circuit for IMPATT diodes," *Solid-State Electron.*, vol. 19, pp. 23–26, Jan. 1976.
[5] H. Okamoto, "Circuit theory of the parametric injection locking of an IMPATT diode oscillator," *Trans. Inst. Electron. Commun. Jap.*, (to be published).
[6] H. Okamoto, M. Ikeda, S. Kodaira, and K. Miyazawa, "Highly stable, low noise millimeter-wave IMPATT oscillator," *IEEE Trans. Microwave Theory Tech.*, (to be published).